Institute of Paper Science and Technology
Atlanta, Georgia

IPST TECHNICAL PAPER SERIES

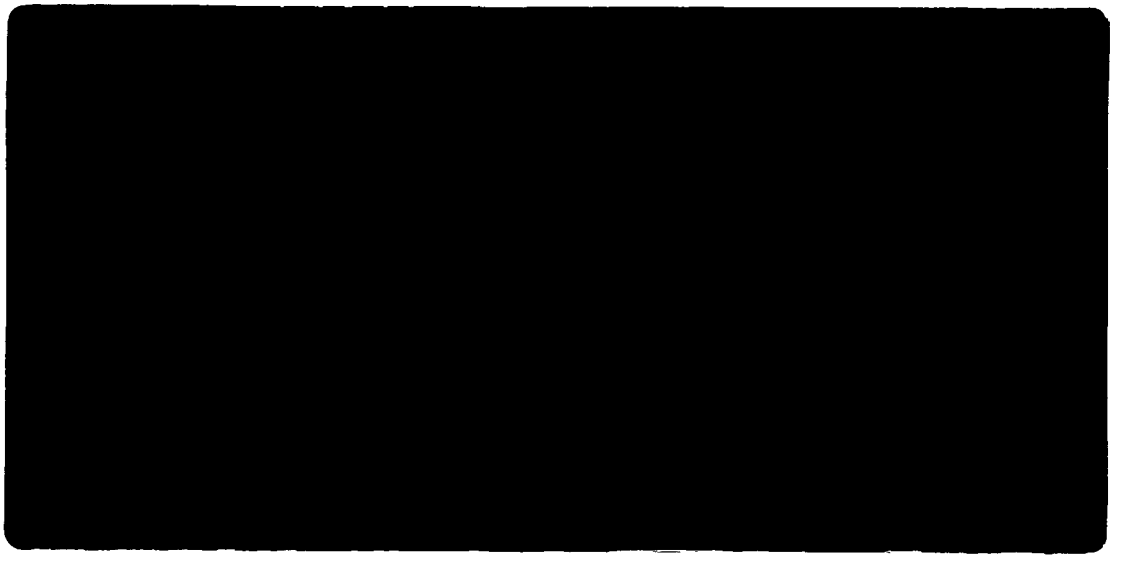

NUMBER 491

AN OVERVIEW OF BLADE COATING SYSTEMS

C.K. AIDUN

JUNE 1993

An Overview of Blade Coating Systems

C.K. Aidun

Submitted to
J. Industrial Coating Research

Copyright© 1993 by the Institute of Paper Science and Technology

For Members Only

NOTICE AND DISCLAIMER

The Institute of Paper Science and Technology (IPST) has provided a high standard of professional service and has put forth its best efforts within the time and funds available for this project. The information and conclusions are advisory and are intended only for internal use by any company who may receive this report. Each company must decide for itself the best approach to solving any problems it may have and how, or whether, this reported information should be considered in its approach.

IPST does not recommend particular products, procedures, materials, or service. These are included only in the interest of completeness within a laboratory context and budgetary constraint. Actual products, procedures, materials, and services used may differ and are peculiar to the operations of each company.

In no event shall IPST or its employees and agents have any obligation or liability for damages including, but not limited to, consequential damages arising out of or in connection with any company's use of or inability to use the reported information. IPST provides no warranty or guaranty of results.

AN OVERVIEW OF BLADE COATING SYSTEMS

Cyrus K. Aidun
Institute of Paper Science and Technology
and
School of Mechanical Engineering,
Georgia Institute of Technology
Atlanta, Georgia 30318

ABSTRACT

This paper provides an overview of blade coating systems with applications to thin-film liquid coating of paper and board. The paper will focus on the more modern pressurized pond application systems. The flow instabilities in the pond and air entrainment at the dynamic contact line will be discussed in more detail. In particular, the three-dimensional behavior of the flow in the pond and at the blade will be discussed.

INTRODUCTION

Blade coating falls within the class of coating systems where the coating layer is metered prior to the meniscus. With this system, the coating liquid passes through a narrow channel which is formed between the blade tip and the substrate (Fig. 1). The flow is primarily due to the shear stress induced by the substrate motion. In contrast to the meniscus-metered class of coating systems where the coating thickness is determined by the meniscus shape, with pre-metered coating systems the coating thickness can be controlled with parameters not dependent on the meniscus.

Similar to many coating techniques, the blade coating technology has evolved from simple and basic applications and cannot be pinpointed to a single technological event or discovery. Many day to day applications are, in principle, forms of blade coating. The simple process of spreading butter by knife over a piece of toast is a simple example. In

fact, Booth (1970) uses this example to describe the effect of coat weight in relation to blade angle.

Blade coating has become the most popular surface application method in manufacturing of coated paper. Other applications include addition of adhesives to paper, board, and film, as well as, application of emulsions onto photographic films and oxide coatings onto magnetic recording tapes.

This simple and rather primitive process presents a complex hydrodynamic system which has been under investigation since its original recognition as a superior coating system as early as the 1950s. Modern blade coating systems operate at speeds in excess of 20 m/sec.
The coating fluid is forced from one extreme to another and the fluid particles experience changes in the shear rate from almost zero upstream of the blade to nearly 10^6 sec^{-1} under the blade in less than a millisecond. Regions with high pressure gradients are adjacent to nearly constant pressure areas (pressure-plateau), and orders of magnitude differences exist in the velocity gradients.

In addition to these complexities, one could hardly design a problem with more complex boundaries. The blade is flexible, the substrate is generally flexible and porous, and there are free-surfaces with static and dynamic contact lines. The expectations for an ideal coating device are also extreme, i.e., the flow needs to remain steady and two-dimensional at high machine speeds for ideal operating conditions.

The first blade coating on a continuous coating machine is attributed to the system designed by Arthur Trist (1945) which was primarily used for coating an oil phase emulsion on bread wrapping paper. The superior potential of this technique was recognized in the 1950s where a growing number of applications started to adopt the blade coating system. A wide variety of blade coating geometries have been invented since then. The earlier systems are reviewed by Richardson (1965) and Booth (1970). There are many forms of blade coating systems which we classify in terms of the mechanical characteristics of the blade and the hydrodynamic characteristics of the application system. In terms of mechanical characteristics, the blade coating systems are divided into *bent* (flexible) and *beveled* (stiff) blade systems (Fig. 2). The application units which apply the coating fluid to the surface of the substrate are located prior to the blade and can be classified into three

categories. These are (*i*) roll, (*ii*) jet, and (*iii*) pond application systems. Each of these application units can operate with a bent or a stiff blade.

Most of the high speed blade coating systems today operate with a roll applicator where a thick layer of coating fluid is transferred to the surface of the substrate. The coating layer which is typically between 100 μm to 1 mm thick is metered downstream by the blade. This operation is sometimes referred to as the *flooded-nip* blade coater. Although this is the most popular blade coating system, it is now clear that other techniques such as jet and pond application systems are superior. These application systems presented schematically in Fig. 3 will be discussed in the next section.

There are several process parameters in a blade coating system which can be adjusted to control the surface quality and thickness of coating applied on the substrate. The various parameters include geometric setting as well as the mechanical or pneumatic load on the blade. The blade thickness is usually between .1 to 1 mm and the blade length is about 2-10 cm.

BLADE COATING: APPLICATIONS

The applicator is where the coating liquid is transferred or applied to the surface of the substrate. This is a critical step in the coating process. There are, in general, three important regions in an application system. (*i*) The *wetting* or the *dynamic contact line* where the fluid first comes into contact with the substrate, (*ii*) the dwell region where the coating liquid remains, usually undisturbed, adjacent to the solid surface, and (*iii*) close to the metering region where the fluid layer approaches the blade.

The flow in an ideal application process should be steady state and two-dimensional. If the coated layer approaching the blade has uniform thickness and if the blade and substrate have no defects, then the resulting coated film would have a constant thickness. However, nonuniformities or unsteadiness upstream of the blade will result in coating defects.

The maximum coating speed is determined primarily by limitations set by the application unit. The fundamental limit on the coating speed depends on the maximum speed at which the air adjacent to the solid surface can be replaced by liquid at the wetting region. This is

sometimes referred to as the maximum wetting speed and depends on the flow field in the vicinity of the dynamic contact line. Above the maximum wetting speed, small air bubbles entrain into the liquid and result in coating defects. Flow instabilities in the application unit upstream of the blade sometimes impose more severe limitations on the coating speed than air entrainment. These instabilities result in operational difficulties and coating defects. Therefore, air entrainment and flow instabilities are the main issues of concern in the development of modern high speed coating systems.

In this section, we review the various coating application methods with respect to their hydrodynamic characteristics.

Puddle-Type Applications

Puddle coaters are one of the more conventional coating systems in operation today. These coaters are simple to operate and can be used for one- or two-sided coating. Fig. 3c shows a schematic of a puddle coater for one-sided coating. For the double-sided puddle coater, better known as the 'Bill-blade' coater, see Fig. 4. Because of air entrainment, foaming, and misting problems, these coaters operate at relatively low speed. The main difference between these coaters and the pressurized pond applicators, described below, is the free surface of the coating liquid inside the reservoir or the 'pond'. The contact (wetting) line at the pond can easily destabilize and lead to air bubbles entraining into the coating liquid. The air bubbles generate problems, including foaming of the liquid and, in some cases, splashing (spouting) at the free surface. In the Bill-blade system, the fluid at the roll side of the pond has two moving boundaries, the web and the roll. The flow forms two eddies and a half-saddle point at the free surface (Fig. 4). When the air entrainment rate at the dynamic contact line becomes excessive, an air channel forms inside the pond, resulting in spouting at the saddle (separation) point of the free surface. The same mechanism could occur in two-roll size presses.

Roll Applicators

This is, perhaps, the most popular and traditional form of coating application. The *transfer or applicator roll* picks up the coating fluid from a supply pan or reservoir, as shown in Fig. 3a, and transfers the fluid to the substrate being carried by the *backing roll*.

The clearance between the surface of the two rolls can vary from 100 μm to 1mm depending on the particular operation. The roll coating modes can be *forward* where the two rolls rotate counter to each other, or *reverse*, where the rolls rotate in the same direction. The amount of coating fluid transferred to the substrate by the applicator roll depends on the fluid properties, the gap, and the relative speed between the substrate and the roll.

There are a number of roll applicator systems with multi-roll metering units which have been developed by various companies. For examples of these systems, the reader is encouraged to see the review by Booth (1970). For a more extensive analysis of the mechanics and instabilities in roll applicators, see Coyle (1992), Savage (1992), and their references.

Roll applicators with blade metering units, in general, provide a good quality coated surface. However, because of flow instabilities and ribbing, roll applicators have limited use in high-speed blade coating. Also, as speed increases, the meniscus splits, forming droplets. This spraying action causes difficulties in maintaining a clean and smooth layer of coating fluid prior to the blade. As indicated above, it is important that the coating layer remains smooth and uniform. A nonuniform layer approaching the blade results in coated film thickness nonuniformities and other defects. In addition to this problem, from a practical point of view, roll applicators are difficult to operate, clean and maintain. Furthermore, light-weight thin film coating requires metering most of the applied coating by exerting a relatively large pressure on the blade. This causes web breaks and blade wear with waste of the coating fluid and the substrate material. Because of these difficulties with roll applicator systems, a number of more advanced application systems are being developed. These fall within the class of jet and pressurized pond application systems.

Jet (fountain) Applicators

This system, as the name implies, consists of a rectangular liquid jet which comes into direct contact with the substrate, as shown in Fig. 3b. We define jet coaters only when the liquid jet emanating from the nozzle directly impacts the substrate. Some in the industry refer to the pressurized pond system of Fig. 3c as jet coaters, as well. However, the fluid flow characteristics and the coating features between the two systems presented

in Figures 3b and 3c are substantially different. With a jet coating system, the entire fluid leaving the nozzle is transferred on the substrate prior to the blade. In contrast, with pressurized pond application system some of the fluid is always rejected from the pond. Also, jet coaters are usually used for thicker liquid film application on the surface. Where thinner film applications can be achieved more efficiently with short dwell time pressurized pond application coaters.

In order to have a uniform coated surface, the jet must have uniform constant momentum across the coater forming a two-dimensional flow. This is achieved, in practice, by injecting the coating fluid from a large reservoir into a long channel before forming the free-surface jet. Since the volume of the reservoir is relatively large, the pressure inside will be essentially static and uniform across the nozzle. A long, slightly converging nozzle will allow the flow to fully develop and prevents the possibility of flow separation.

The control parameters are the opening gap of the jet, d, the jet angle relative to the substrate, α, the velocity of the substrate, U, the jet Reynolds number, $\mathrm{Re} \equiv \frac{\rho d V}{\mu}$, and the capillary number, $\mathrm{Ca} \equiv \frac{\mu V}{\sigma}$ where ρ, μ, and σ are the fluid density, viscosity, and surface tension, respectively. The jet velocity scale, V, is defined as the mass flux divided by the jet's cross-sectional area. It is well known that the jet could swell or contract depending on Re and Ca.

With jet coaters, the entire coating liquid which is ejected from the nozzle remains on the surface of the web. Therefore, it is important to remove any air bubbled from the coating liquid prior to application. Furthermore, the jet angle, α, and the jet velocity, V, have to be adjusted and optimized with respect to the substrate velocity, U, in order to prevent air entrainment from the contact line.

Pressurized Pond Application

Most of the developments in blade coating systems are associated with the application method. The pressurized pond application systems are the most modern developments in blade coating. The first of these systems, known as short-dwell time application coater, (short-dwell coaters, DC) were developed in the 1970s. It is a modification of the puddle coater where the free surface is replaced by a solid boundary and the flow is injected

through a slot at the bottom of the pond. Similar to puddle coaters, the blade is placed adjacent to the pond. The coating liquid can escape the pond at the blade tip or the 'overflow baffle,' as shown in Fig. 3d.

In contrast to the long-dwell time coaters (e.g., flooded nip with roll, Fig. 3a, or pond applicators, Fig. 3e) where the coating layer travels adjacent to the substrate for a relatively long time before being metered off, the coating liquid in short-dwell coaters, Fig. 3d, have little time to penetrate into the substrate. These coaters have several advantages over other coating application systems. The main advantages are the compactness, operational efficiency, and increased productivity of light weight (i.e., low coated film thickness) coated layers in the range of 5 to 10 μm (based on 1200 kg/m^3 density of the coating liquid).

More recently, the pressurized pond application system has been used in a long-dwell time mode (Fig. 3e). Here, the coating is applied with a bent blade and the excess is scraped off at a downstream location with a beveled blade. This is similar to the flooded nip system where the roll applicator is replaced by a pond application unit.

These coaters are primarily used on-line (i.e., at the final stage of the paper machine) in production of light-weight coated printing papers. Depending on the coating liquid rheology, these coaters can operate up to about 20 m/sec. In general, above this speed the film thickness looses its uniformity and a streaking pattern appears on the coated surface. These problems are associated with the instabilities that occur inside the pond as well as air entrainment issues at the dynamic contact line. These issues are treated in the next section.

CAUSES OF MACROSCOPIC BLADE COATING DEFECTS

In this section, we review some of the hydrodynamic mechanisms which result in macroscopic coating defects. Here we exclude defects with length scales in the order of the blade gap (~50 μm). There are a number of ways that flow instabilities in the application zone upstream of the blade can cause film thickness nonuniformities. These are summarized in Fig. 5. Starting with air entrainment issues, we will briefly discuss each of these mechanisms and outline the most likely systems where these problems could occur.

Air entrainment at the overflow baffle proposed by Aidun (1989) is one of the prime candidates. The recent pilot coater experiments by Li and Burns (1992) show a decrease in the streaks as the air accumulated inside the pond is removed. We emphasize that this mode of air entrainment in the form of air bubbles entering and accumulating inside the pond occurs at machine speeds lower than the speed resulting in skip coating where a continuous air layer (or channel) extends from the overflow baffle to the blade preventing contact between the coating liquid and the substrate.

There are considerable information and correlations on the critical speed for the onset of air entrainment in the plunging tape experiments (see Burley, 1992 and references. Also, Scriven, 1982 and references). The sequence of events leading to excessive air entrainment in the form of small bubbles from a dynamic contact line formed by a rotating roll half-way immersed in a pool of liquid is revealed by Veverka and Aidun (1991) and Aidun et al. (1991b). None of these studies, however, have been able to explain the physics of air entrainment. For example, why increasing the liquid viscosity would decrease the critical speed for the onset of air entrainment? What determines the structure and the length scale of the V-shaped patterns? Do these structures appear as a result of instability (a symmetry breaking bifurcation) of the dynamic contact line?

Air entrainment in high-speed coating systems where the fluid is forced against the substrate under pressure, as in the case of a short-dwell coater or a roll applicator, has remained virtually unexplored. As an example, lets consider the flow at the overflow baffle of a short-dwell coater where a half-saddle point resides on the free surface near the contact point. The air entrainment speed in this case is much higher than the plunging tape or other low pressure wetting or coating situations. However, it is now well established that air inclusions inside the coating liquid is partly responsible for coating defects.

The macroscopic coating nonuniformities usually occur in the form of streaking patterns which could be randomly distributed along the coated area. More regular patterns are also common with a certain class of coating applicators.

The most troublesome coating defects in recent years has been associated with pressurized pond applicators. This is perhaps the main reason that these systems have not been able to fully replace the roll applicator flooded nip systems. In general, the quality of roll

applicators are better than the pond applications. However, because of the ever increasing demand for light-weight coated paper, pressurized pond coaters have gained considerable popularity over the past decade. Although the most popular system in this class of coaters is the short-dwell coater, the discussion in this section would equally apply to other pressurized pond application systems with recirculating eddies inside the pond.

With these systems, the flexible blade acts both as a boundary of the coating color reservoir and as a metering unit (Fig. 3c, d, and e). These systems have advantages of compactness, low color penetration, long blade life, and less sheet break due to low blade loading. But movement toward further increase of coating speed has been hindered by difficulty in maintaining uniform coat-weight profile in the CD. In its extreme case, an uneven coat-weight profile appears as a patterned surface characterized by streaks of 1 to 3 cm wide running along the machine direction (MD). We should note that this length scale (~1 cm) is orders of magnitude larger than the blade gap (30-50 μm) and that these streaks have, in general, less coat weight than the rest of the coated surface. The streaks are estimated to have 15 to 50 percent deficit in coat-weight relative to the rest of the coated surface. This is in contrast to streaks caused by a solid particle blocking the blade gap, or skip coating, where the streaks essentially have no coating. Wet streaks occur when the machine speed increases above a critical limit for a given coating color viscosity. Pilot coater trials (26,17) show that this limiting speed decreases by increasing the percentage solids, and consequently, the low-shear viscosity of the coating color.

Experiments with Newtonian fluids and a through-flow lid-driven cavity simulating the pond of a short-dwell coater (4,8) revealed the sequence of transitions from steady state (SS) to time-periodic (TP), and eventually, a state with more than two fundamental frequencies (see Fig. 6) referred to, from now on, as the "unsteady state." This state seems to follow a quasi-periodic state (QP) at Re = 1000 and is characterized by a broad band of frequencies.[1] The mushroom-shape structures which appear at the unsteady state (Fig. 6d) could be an initial state of Görtler-like vortices observed by Koseff and Street (1984c) in a confined lid-driven cavity flow at Re = 3200. It is important to note that the length scale of the mushroom-shape vortices (Fig. 6d) is the same as the width of the wet

[1] The measurements by Benson and Aidun (4) suggest a SS→TP→QP→chaotic sequence of transitions. Rigorous stability analysis is required to map the transitions more accurately and to establish the sequence of instabilities to unsteady nonperiodic (chaotic) flow.

streaks discussed above. Also, the dynamical characteristics of the streaks correspond to the rapid motion of these structures in the pond. Based on these observations, we conclude that these structures are an important factor in generating the streaks (for more detail see Aidun, et al. 1991a).

The fourth mechanism in Fig. 5 is based on pressure variations upstream of the blade. A three-dimensional (3-D) flow upstream of the blade results in some variations in the static pressure at the blade gap entrance. Since a portion of the mass transfer into the blade gap is pressure driven, the variation in static pressure could result in coat-weight variations. We (Miura and Aidun, 1992) have examined the importance of temporal as well as spatial pressure variations in the cross-machine (spanwise) direction by solving the full equations governing the transient 3-D flow at the blade. All of the previous computational analyses of blade coating assume no flow or variations in the third dimension. A two-dimensional (2-D) analysis can be extremely useful in terms of predicting an average coat-weight and investigating the various blade coating features, such as substrate and blade deformation (21,22), coating color penetration into the substrate (11), and design of new coating application systems (2). Conclusions made from 2-D computations without including a stability analysis, however, could be somewhat misleading. We now know that the solution of a steady 2-D flow in the pond of a short-dwell coater represents a solution branch which is locally unstable to a time periodic state at Re > 900 (4). Therefore, the 2-D steady state solutions reported in previous studies (1, 12,27,28) are unstable to infinitesimal disturbances and do not represent a physical flow at Reynolds number above 900.

Linear stability analysis of 2-D flows in slide coating (13) have proved to be quite effective. However, to investigate the magnitude of the meniscus nonuniformity in the spanwise direction due to pressure variations upstream of the blade gap, Miura and Aidun (1992) have solved the full transient 3-D flow equations. Including the third dimension in the analysis increases the computational cells by an order of magnitude. The added complexity of solving the strongly nonlinear interfacial conditions at the free surface, which now has two radii of curvatures, demands a careful setup of the domain and the boundary conditions for a most efficient, and therefore, tractable problem. Since the main objective in this study was to determine the significance of coat-weight variations caused by the pressure fluctuations upstream the blade, they considered a nonporous smooth substrate (e.g., the backing roll) and neglected the deformation of the substrate and the

blade. This will isolate the effects of the third feature introduced by Fig. 5, that is, nonuniform deformation of the substrate and the blade gap opening.

The modified volume-of-fluid technique (16) is used to solve the 3-D flow of a highly viscous coating fluid at the blade. The flow at the entrance side of the blade consists of a shear-driven (Couette-flow) and a pressure-driven (Poiseuille-flow) component (21,22).

The web speed, W, the blade gap, h, the convective time scale, h/W, and $\mu W/h$ are used for the velocity, length, time, and pressure scales, respectively. From here on all of the variables shall be considered as dimensionless unless otherwise stated.

Fig. 7 represents the computational domain and the grid system. Note that the vertical direction is greatly scaled up in this and the following figures.

The inlet velocity boundary condition at the blade gap (Fig. 7a) consists of Couette- and Poiseuille-flow components given by

$$w(x,y,t) = 1 - x + \frac{1}{2}\frac{dp}{dz}(x-1)x \qquad \text{at} \qquad z=0 \tag{1}$$

where the pressure gradient, $\frac{dp}{dz}$, can be a function of spanwise position, y, and time, t. The problem considered here has two parameters, namely the Reynolds number, $R = \rho Wh/\mu$, and the capillary number, $Ca = \mu W/\sigma$.

Analysis of flow at the blade nip involves mathematical treatment of a deforming meniscus and a static contact point at the exit side tip of the blade. Local analysis of the flow near the static contact point shows that the discontinuity in shear and stress results in a mathematical singularity in the continuum approximation. This results in pressure and velocity gradients increasing without bound as $r^{-1/2}$, where r is the distance from the static contact point. The contact angle at this point is a major factor influencing the shape of the meniscus. We treat this point in a special manner. The point is fixed at the sharp corner of the solid, and the contact angle is determined from the equations and the interfacial conditions. We have done a thorough examination of our technique for accuracy by solving the various free-surface test problems including the well-known die-swell problem and comparing the results with the literature. The results are reported by McKibben and Aidun (16).

The flow instability upstream of the blade results in pressure gradient variations in the spanwise (cross-machine) direction. The purpose of the 3-D computations, presented in this section, is to investigate the importance of the static pressure fluctuations on the film thickness nonuniformity. Depending on the type of flow instability, the wavelength of the pressure variation could vary from a millimeter to about a centimeter or more.

The effect of film thickness nonuniformities is most important in light-weight coating where the blade gap is about 30 μm. The dimensionless parameters and a typical dimensional value used for the 3-D computations are listed in Table I. The Reynolds number and Capillary number fall within the range of actual operating conditions. Although coating fluids are usually shear thinning, here we assume a constant viscosity based on the typical value at high-shear rates in the order of 10^6 1/s. The average value of the pressure gradient at the blade nip inlet is estimated from the finite element computations by Pranckh and Scriven (21) which is currently the most complete analysis of 2-D blade coating.

Table I. Boundary and flow parameters for the three-dimensional computation.

Parameter	Dimensionless	Dimensional
Speed of substrate, W	1	20 m/s
Blade gap, h	1	$3x10^{-5}$ m
Blade thickness, τ	33.33	$1x10^{-3}$ m
Density, ρ	—	1200 kg/m^3
Viscosity, μ	—	.05 Pa.s
Surface tension, σ	—	.05 N/m
Average pressure gradient, <dp/dz>	1.44	$-1.6x10^9$ Pa/m
Reynolds number, R	14.4	—
Capillary number, Ca	20	—

The pressure fluctuation in the y-direction is approximated as a sinusoidal variation given by

$$\frac{dp}{dz} = \left|\frac{dp}{dz}\right|\left[1 + 0.5\cos\left(\frac{n\pi y}{Y}\right)\right] \qquad (2)$$

where $\left|\frac{dp}{dz}\right|$ indicates spatial average of pressure in the y-direction, and Y is the pressure fluctuation wavelength. The value of n could be 1 or 2, representing half-wave or full-wave fluctuations, respectively.[2] The pressure is allowed to vary by 50% in magnitude. All of the boundary conditions remain as before with the addition of symmetry plane conditions imposed at the side walls, such that

$$u = \frac{\partial v}{\partial x} = \frac{\partial w}{\partial x} = \frac{\partial p}{\partial x} = 0 \qquad \text{at} \qquad y = \pm Y/2 \qquad (3)$$

In this series of computations, the main parameter is the span length, Y, which is varied from 33.3 to 400 corresponding to a dimensional length of 1 mm to 1.2 cm. All of the 3-D simulations start from a 2-D base case solution where only the two-dimensional equations are solved. For the 2-D base case, the contributions to the film thickness from the shear-driven flow (Couette-flow) and pressure-driven flow (Poiseulle-flow) can be determined by integrating Eq. (2). The total film thickness is given by

0.5	+	.12	=	0.62
Couette-flow contribution		Poiseuille-flow contribution		Total

The film thickness predicted by computationally solving the base 2-D case is 0.6206 which is accurate enough for all practical purposes. The computed pressure adjacent to the substrate (i.e., at x = 0) is plotted in Fig. 9. Results show a negative pressure at the blade tip which agrees with the results from parallel blade setting computed by Pranckh and Scriven (1988;1990).

---

2 In our analysis, we have considered cases with a full-wave of pressure fluctuation to examine any remote possibilities of symmetry breaking instabilities. None of the cases considered in this study, however, became unsymmetric.

In summary, the results are as follows. Comparing the film thickness profiles for 50% spanwise sinusoidal pressure variations with wavelengths, Y, of 33.3 (1 mm), 100 (3 mm), 200 (6 mm), and 400 (12 mm) shows (Fig. 9) that the nonuniformity in the film thickness profile increases significantly with the spanwise length of pressure variation. This is despite the fact that the magnitude of the pressure gradient is the same for all Cases. 50% variation in pressure gradient results in film thickness variation of less than 1% for 1 mm span and more than 15% for 1.2 cm span. The percentage variation in the rate of increase in the film thickness nonuniformity is maximum when Y is changed from 1 mm to 3 mm, and it decreases from 6 mm to 1.2 cm. This observation indicates that there is a critical wavelength at about 2-4 cm which corresponds to the maximum film thickness nonuniformity.

The study by Miura and Aidun (1992) is the first 3-D simulation to analyze the effect of pressure fluctuations upstream of the blade on coat-weight nonuniformities downstream of the blade. The primary result of this work is that the width of the domain, where pressure fluctuation is applied, greatly influences the magnitude of the film thickness variation for the parameters considered. In other words, a wider region of pressure fluctuation causes greater coat-weight nonuniformities. Although in this study the deformation and water absorption of the web and viscosity variation has not been considered, the results provide important information regarding the large-scale streak patterns due to pressure fluctuations upstream of the blade.

Another important implication of the results of this study is the possibility of substrate deformation (i.e., combination of the web and the rubber layer of the backing roll) resulting in coat-weight nonuniformities. Although substrate deformations are not considered in this work, the results of pressure profiles in Fig. 9 show great spanwise variations on the web under the blade. This could cause coat-weight nonuniformities due to nonuniform deformation of the web and the rubber layer as discussed for the two-dimensional case by Pranckh and Scriven (1989), and for the three-dimensional effects by Aidun (1991), and Miura and Aidun (1992), and the experiments by Ortman and Donigian (1992) which clearly demonstrates the significance of the substrate deformation in promoting coating film nonuniformities. In their experiments, Ortman and Donigian (1992) examine a flooded nip coater with an applicator roll. They showed that by using a harder roll, they could eliminate the streaks in the coating operation. It should be noted that this mechanism applies most significantly to roll applicator flooded nip systems.

CONCLUSIONS

By way of summarizing the causes of coating defects, we outline a strategy for detecting and removing the macroscopic defects in blade coating systems. The following flow chart could be useful in determining the origin of a defect and possibly removing it from the process.

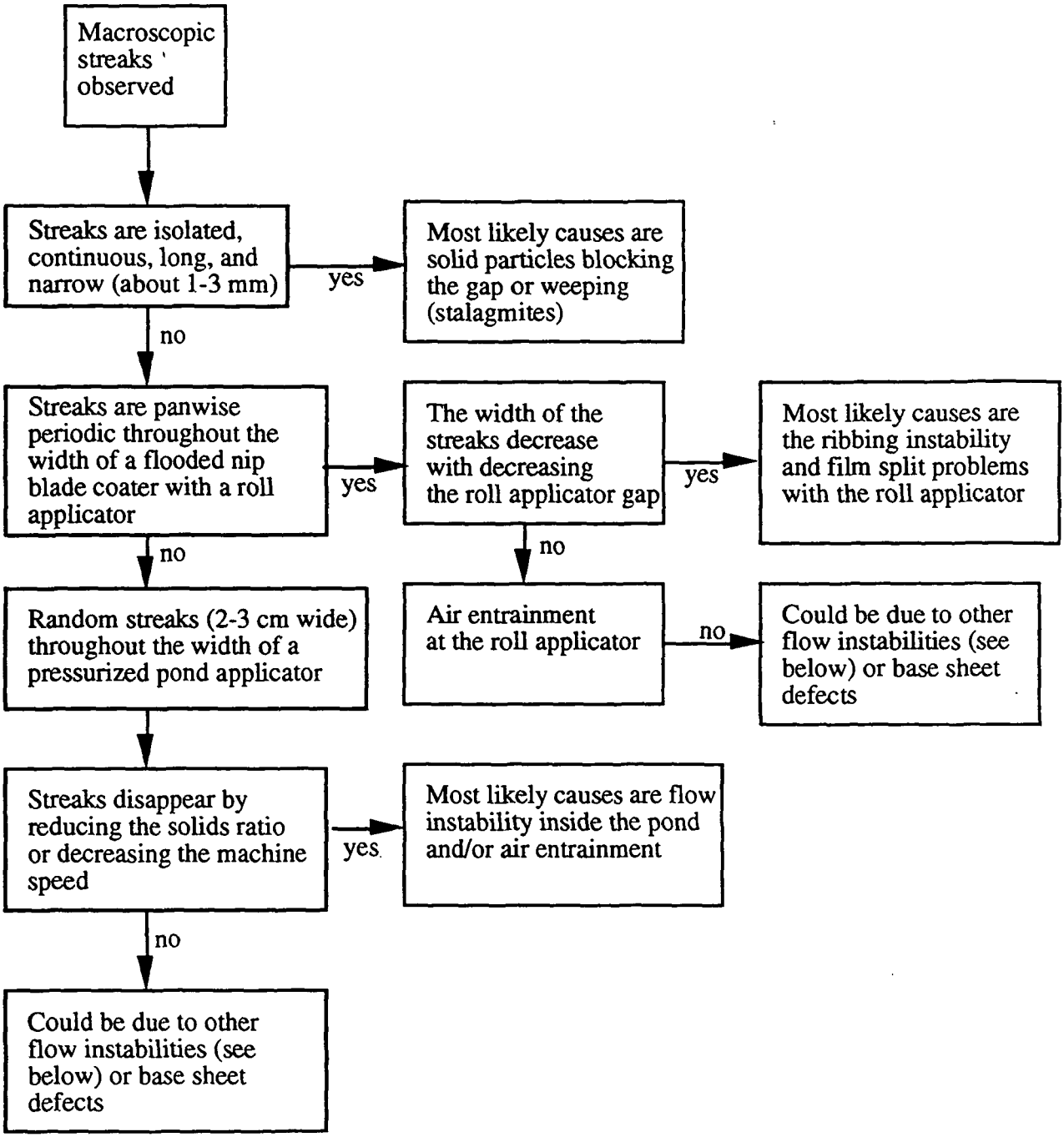

There are several kinds of flow instabilities that could become important in blade coating systems. These are described in [6] and summarized below by Figures 10 and 11.

ACKNOWLEDGMENTS

This work has been supported in part by the National Science Foundation's Young Investigator Award under grant CTS-9258667 and by matching contributions from Beloit R&D Center, Union Camp Corp., Westvaco Corp., ECC International, Blandin Corp., and Tappi Foundation.

LITERATURE CITED

1. H. Affes, A. T. Conlisk, and M. R. Foster, "The Steady Flow in a Short-Dwell Coater" Proc. TAPPI Coating Conference, TAPPI Press, Atlanta, GA, p. 299 (1990).

2. C. K. Aidun, "A Vortex-Free Short-Dwell Coater" Report to Engineering Project Advisory Committee, Institute of Paper Science and Technology, (1992).

3. C. K. Aidun, "Fundamentals of Coating Systems" Report to Engineering Project Advisory Committee, The Institute of Paper Chemistry, (1989).

4. C. K. Aidun, N. G. Triantafillopoulos, and J. D. Benson, *Phys. Fluid A,* "Global Stability of a Lid-Driven Cavity with Throughflow: Flow Visualization Studies" 3: 2081 (1991).

5. C. K. Aidun, P. J. Veverka, and L. E. Scriven, "Onset of Air Entrainment: Mechanism" AIChE Annual Meeting, November 17-22, (1991).
Also, C.K. Aidun, P.J. Veverka, and L.E. Scriven, "Interfacial Instability And Excessive Air Entrainment," Presented at the 6th International Coating Process Science and Technology Symposium, AIChE National Meeting, New Orleans, LA, U.S.A., March 29 - April 2, 1992

6a. C.K. Aidun, "Flow Characteristics in Coating Applications," *Proc. IPST Executives' Conf.*, 11-17, May 1-2, 1991a.

6b,c,d. C.K. Aidun, "Principles of Hydrodynamic Instability: Applications to Coating Systems -- Part I: Background," *Tappi J.*, **74** (2), 213, 1991b.
Part II: Examples of Coating Flow Instability," *Tappi J.*, **74** (3), 213, 1991c.
Part III: Generalization of Coating flows as Dynamical Systems," *Tappi J.*, **74** (4), 209, 1991d.

7. R. Burley, "Mechanisms and Mechanics of Air Entrainment in Coating Processes," *J. Industrial Coating Research*, **2**, 95-108, 1992.

8. J. D. Benson and C.K. Aidun, "Transition to Unsteady Nonperiodic State in a Through-Flow Lid-Driven Cavity," *Phys. Fluid* A, **4** (10), 2316, 1992.

9. G. L. Booth, Coating Equipment and Processes, Lockwood Publishing Co. Inc., 551 Fifth Ave., New York, 1970.

10. Eklund, D.E., "Review of Surface Application," Trans. of the Ninth Fund. Research Symp., ed. Baker and Punton, Mech. Eng. Pub., 1989.

11. K. S. A. Chen and L. E. Scriven, "On the Physics of Liquid Penetration into a Deformable Porous Substrate" Proc. TAPPI Coating Conference, TAPPI Press, Atlanta, GA, p. 93, (1989).

12. A. T. Conlisk and M. R. Foster, "The Steady Flow in a Short-Dwell Coater II" Proc. TAPPI Coating Conference, TAPPI Press, Atlanta, GA, p. 327 (1991).

13. K. N. Christodoulou and L. E. Scriven, *J. Fluid Mech.,* "The Fluid Mechanics of Slide Coating" **208**, 321 (1989).

14. D. J. Coyle, "Roll Coating Flows II: The Ribbing Instability," *Industrial Coating Research*, **2** (1992) 33-45.

15a. Koseff, J.R., and Street, R.L., "Visualization Studies of a Shear Driven Three-dimensional Recirculating Flow," *J. Fluid Eng.*, **106**, 21, 1984a.

15b. Koseff, J.R., and Street, R.L., "On end wall effects in a Lid-Driven Cavity Flow," *J. Fluid Eng.* **106**, 385, 1984b.

15c. Koseff, J.R., and Street, R.L., "The Lid-Driven Cavity Flow: a Synthesis of Qualitative and Quantitative Observations," *J. Fluid Eng.*, **106**, 390, 1984c.

16. J. F. McKibben and C. K. Aidun, "A Volume-of-Fluid Computational Technique for Free-Surface Flow Problems," submitted for publication (1993).

17. A. Li, Personal Communication, (1990).

18. A. Li and J. Burns, Personal Communication, (1991).

19. H. Miura and C.K. Aidun, "Pressure Fluctuations and Coat-Weight Nonuniformities in Blade Coating," *Proc. Tappi Coating Conference*, 193-216, 1992.

20. B.J. Ortman, and D.W. Donigian, "Coat-Weight Nonuniformity Due to High-Speed Blade Coating: Mechanism and Prevention," *Proc. Tappi Coating Conf.*, 217-239, 1992.

21. F. R. Pranckh and L. E. Scriven, "The Physics of Blade Coating of Deformable Substrate" Proc. TAPPI Coating Conference, TAPPI Press, Atlanta, GA, p. 217, (1988).

22. F. R. Pranckh and L. E. Scriven, *AIChE J.,* "Elastohydrodynamics of Blade Coating" 36: 587 (1990).

23. C.A. Richardson, "The trailing Blade Coater," *Tappi*, **40**, No. 8, 1957.

24. M.D. Savage, "Meniscus Instability and Ribbing," *Industrial Coating Research*, **2** (1992) 47-58.

25. A.R. Trist, U.S. Patent 2,368,176, 2,593,074 and 2,796,846, 1945.

26. N. G. Triantafillopoulos and C. K. Aidun, *Tappi J.*, "Relation Between Flow Instability in Short-Dwell Ponds and Cross Directional Coat Weight Nonuniformities" 73: 127 (1990).

27. N. G. Triantafillopoulos, G. R. Rudemiller, T. Farrington Jr., and J. D. Lindsay, "Numerical Simulation of Short-Dwell Coater Pond Flows" Proc. TAPPI Coating Conference, TAPPI Press, Atlanta, GA, p. 209, (1988).

28. N. G. Triantafillopoulos, G. R. Rudemiller, and C. K. Aidun, "Fluid Dynamics of Short-Dwell Coater Pond Flows, Numerical Simulation" Int'l Symp. Coating Structures and Rheology, INSKO, Helsinki, Finland, 1989.

29. L.E. Scriven, "How Does Air Entrain at Wetting Lines," presented at the International Symposium on Thin Film Coating, AIChE Spring National Meeting, Orlando, FL. (1982).

30. P. J. Veverka and C. K. Aidun, "Flow Visualization of Air Entrainment and Dynamic Contact Line Instability in Low-Speed Roll Coating" Proc. TAPPI Engineering Conference, TAPPI Press, Atlanta, GA, 2: 719 (1991). Also, Tappi J., 74 (9), 203, 1991.

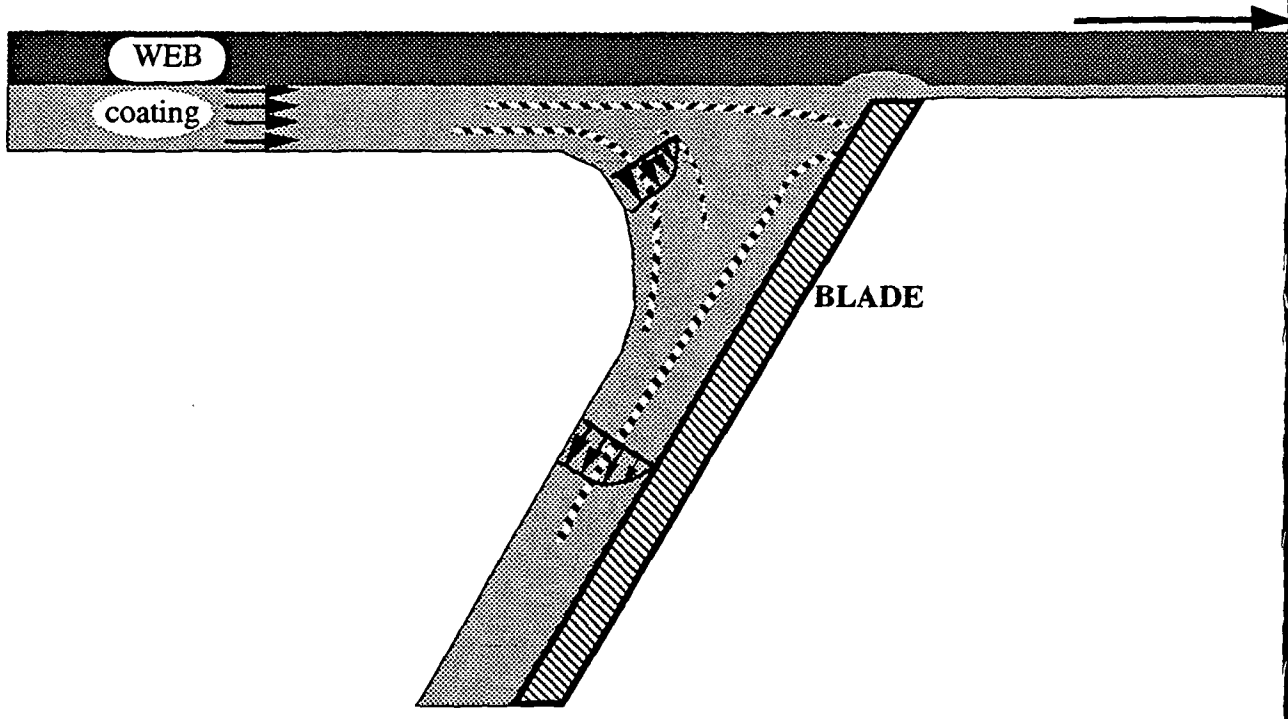

Figure 1. Schematic of a flooded-nip blade coater.

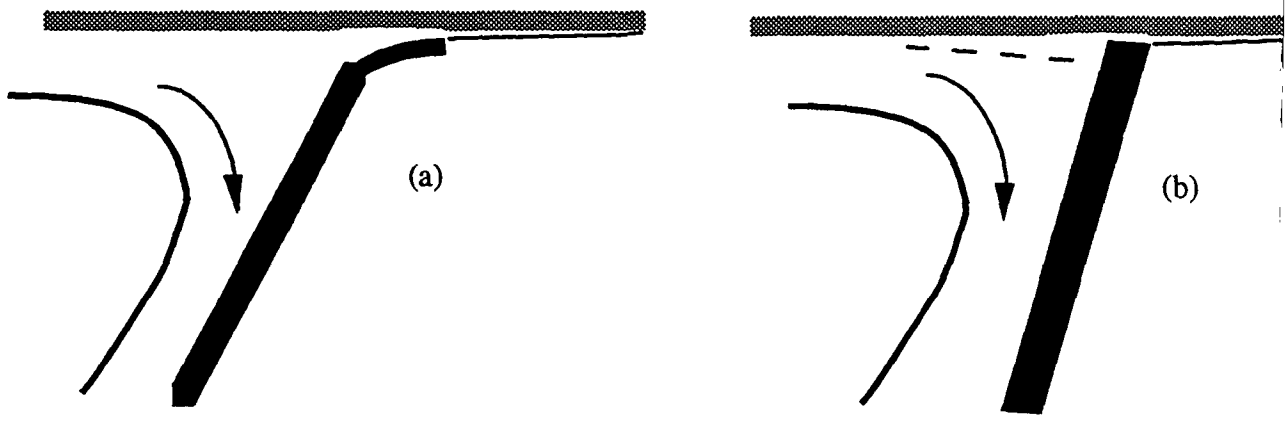

Figure 2. Schematic presentation of (a) bent and (b) bevelled blade coater.

(a) Roll applicator

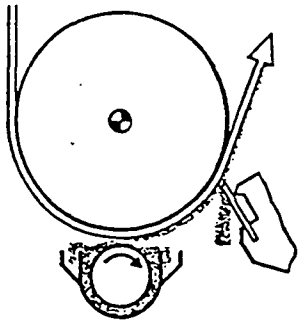

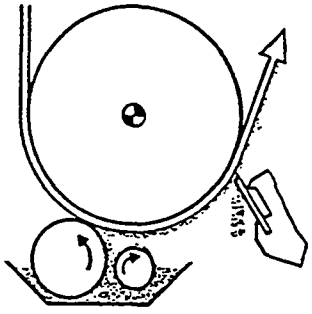

(b) Jet application

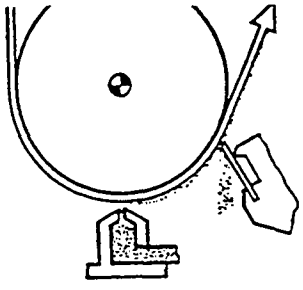

(c) puddle coater

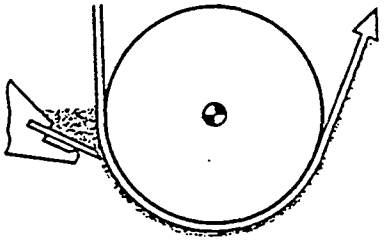

Figure 3. see next page for caption.

(d) short-dwell coater

(e) pond applicator

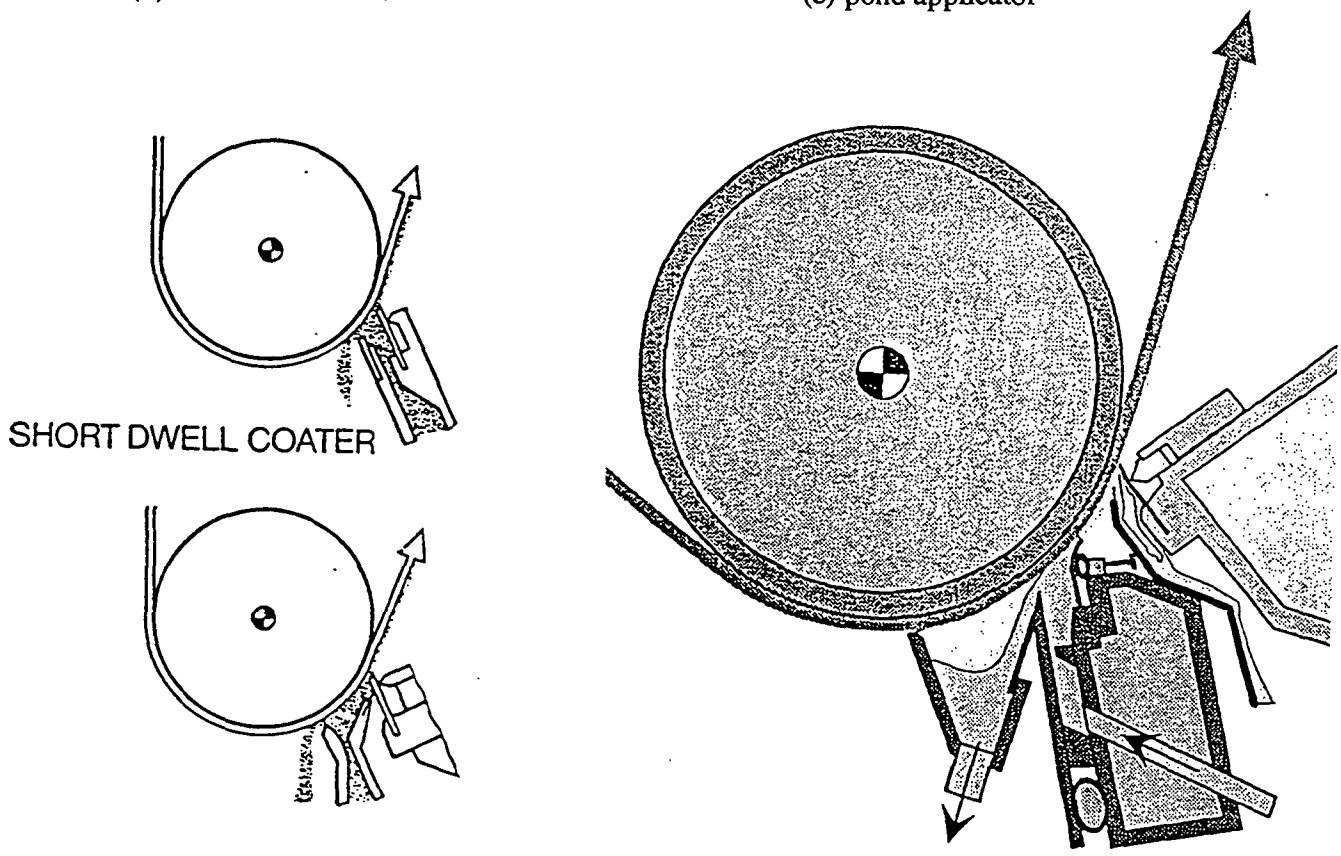

Figure 3. Schematic of (a) roll, (b) jet, and pond application systems which include (c) puddle coater and pressurized pond application systems with (d) short-dwell time and (e) long-dwell time modes of operation.

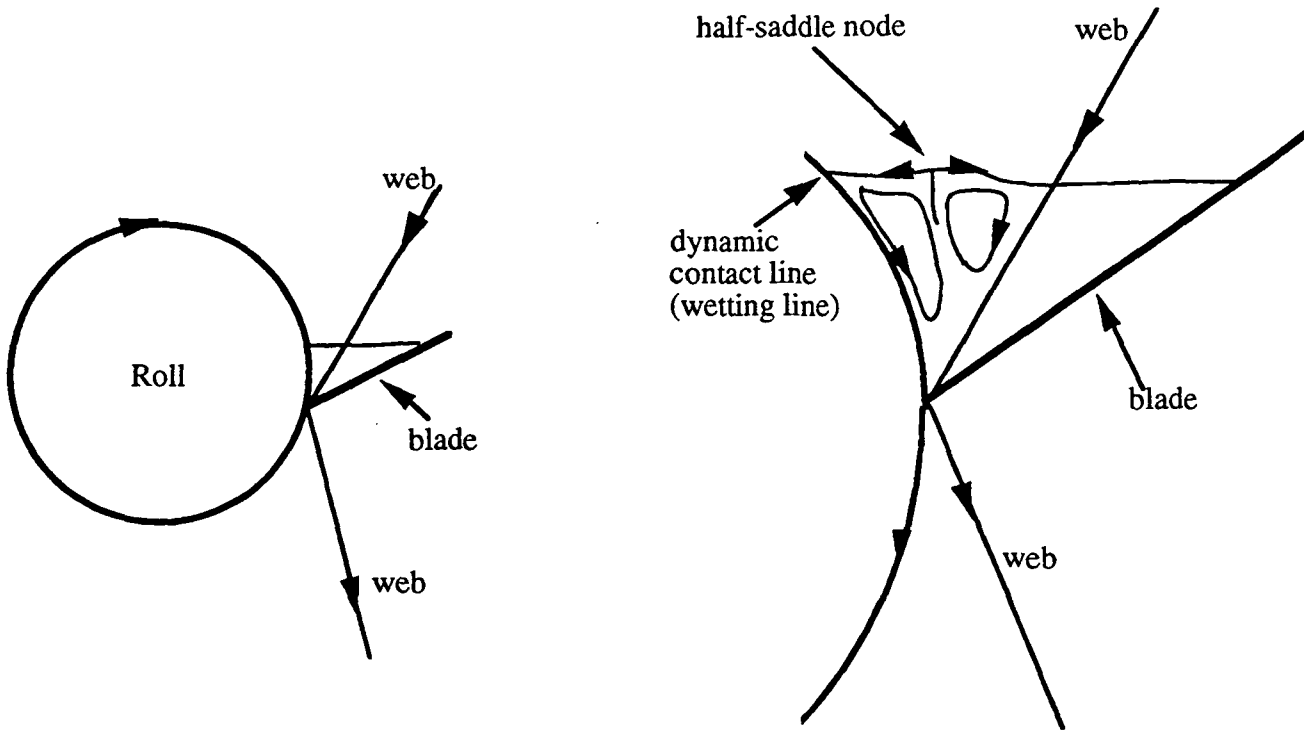

Figure 4. Double-sided puddle or (Billingsfors-Langed) Bill-blade coater.

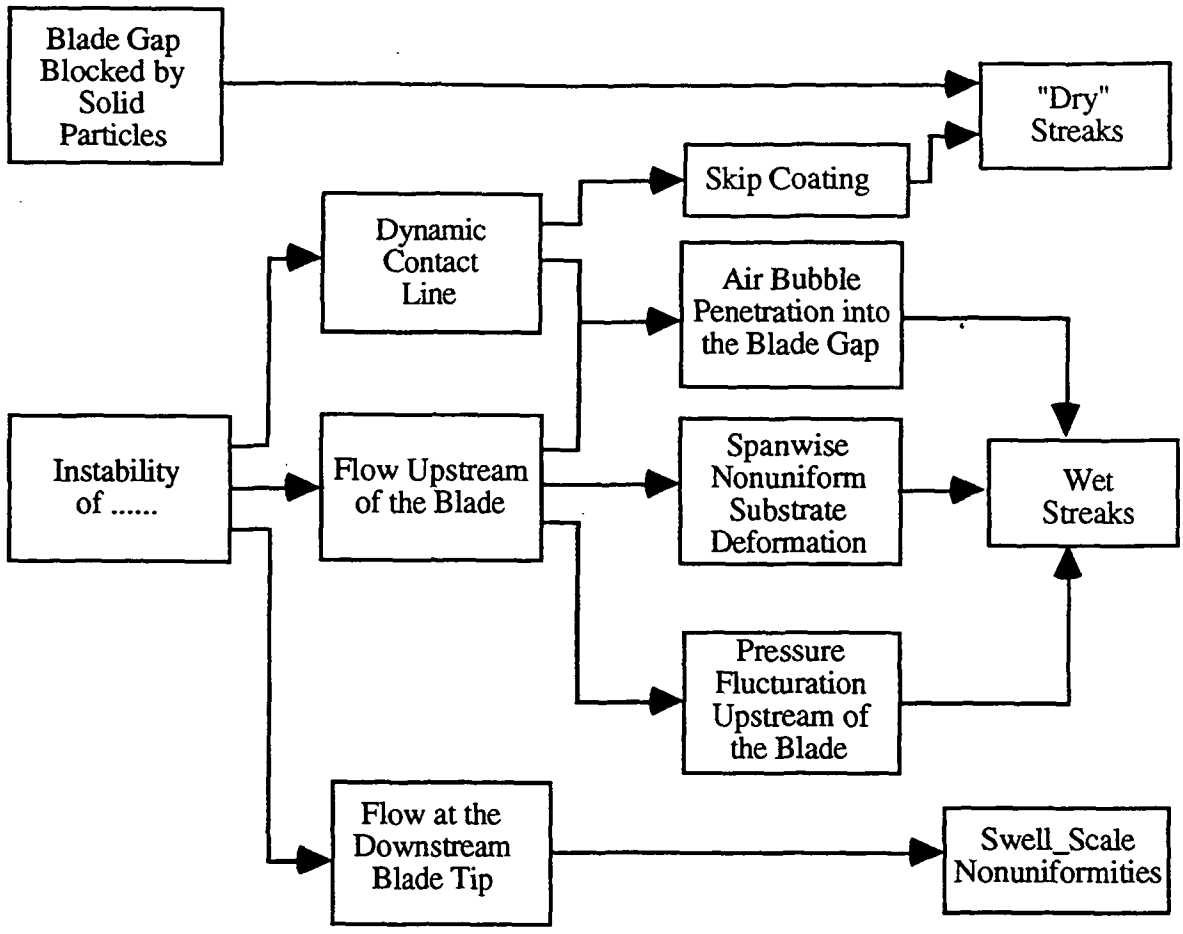

Figure 5. The mechanisms and origins of macroscopic coating defects.

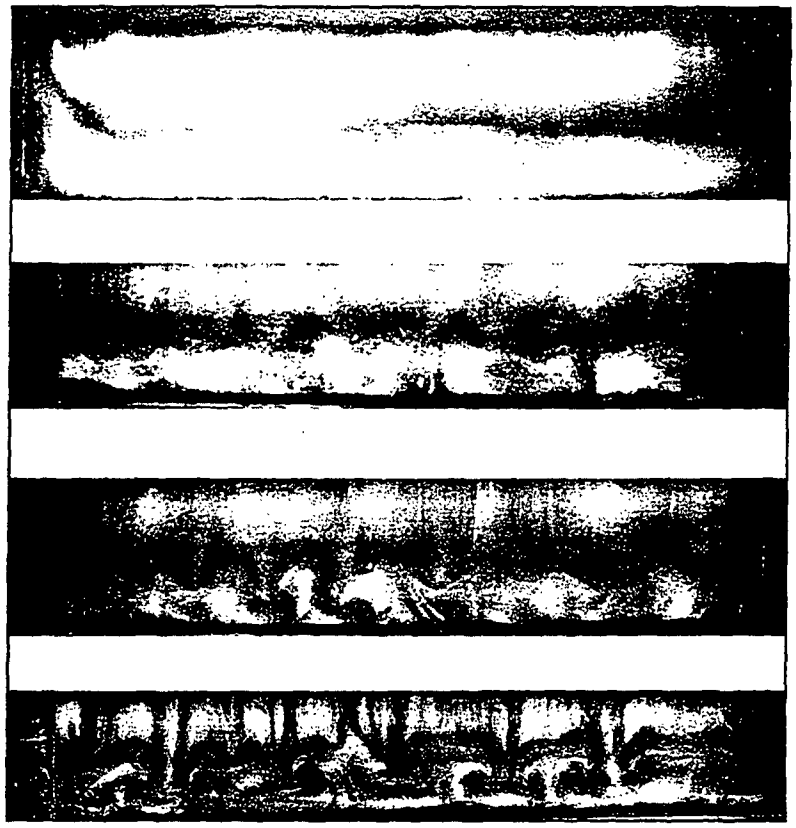

Figure 6. Sequence of instabilities and transition in a pond simulating a short-dwell coater; (a) one-cell steady state, Re~500; (b) time periodic state, Re~900, (c) downstream secondary eddy starts to fold Re~1200, and (d) chaotic state, Re>1900.

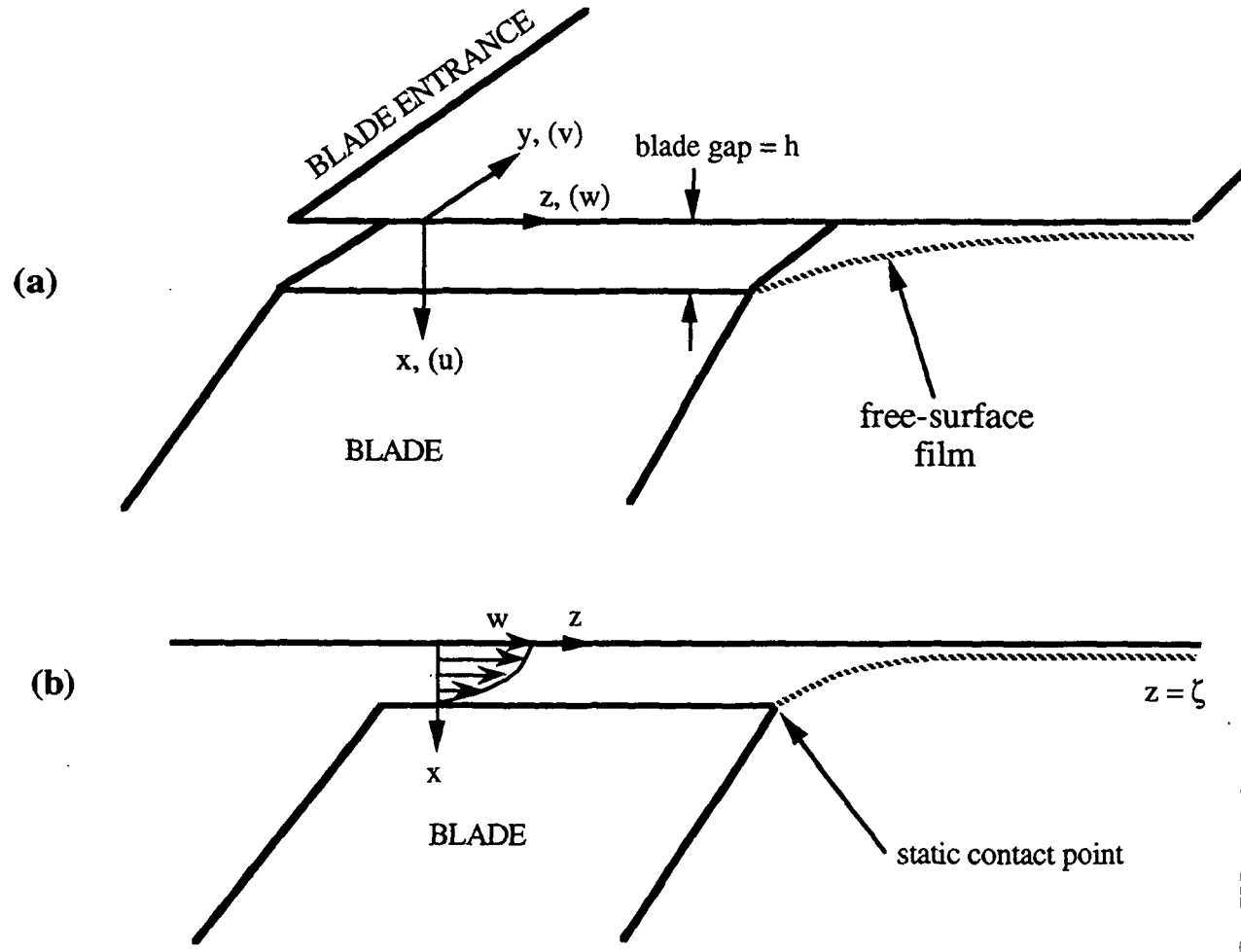

Figure 7. Illustration of the (a) blade geometry and the coordinate system, and (b) two-dimensional cross-section of the domain.

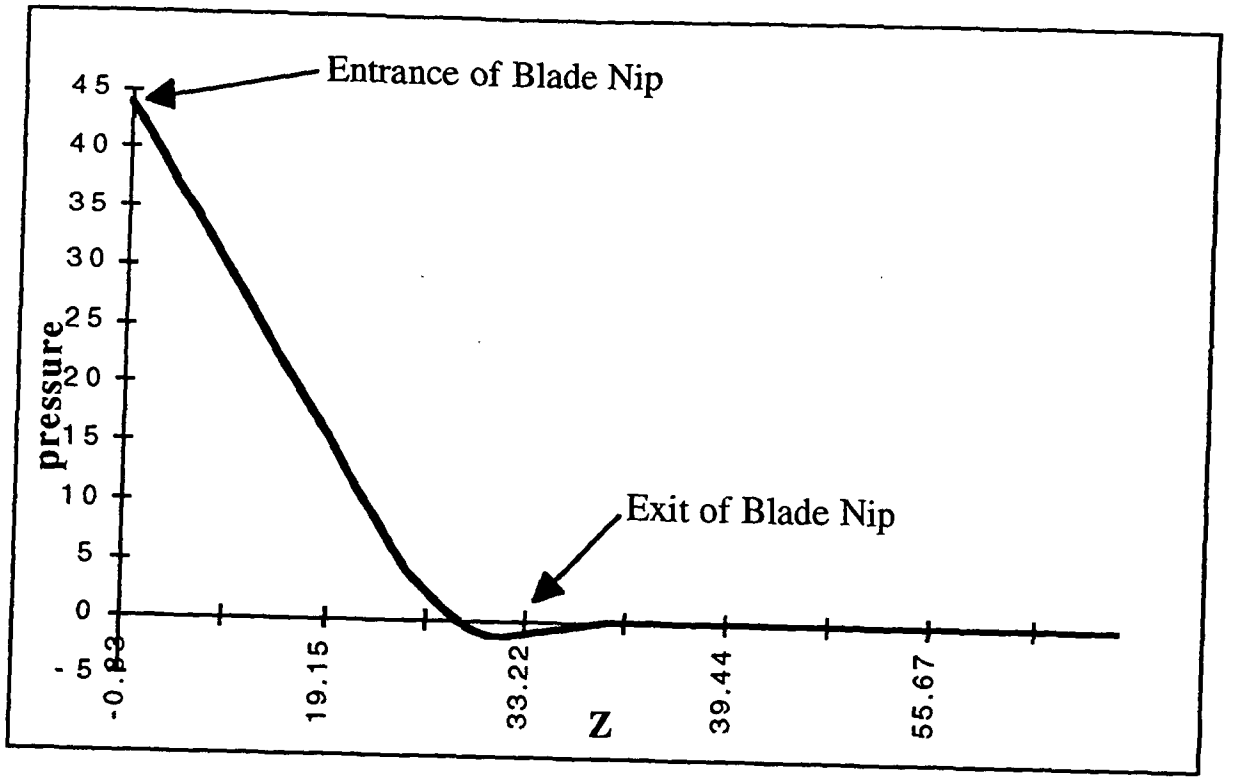

Figure 8. Pressure profile adjacent to the substrate (i.e., at x=0).

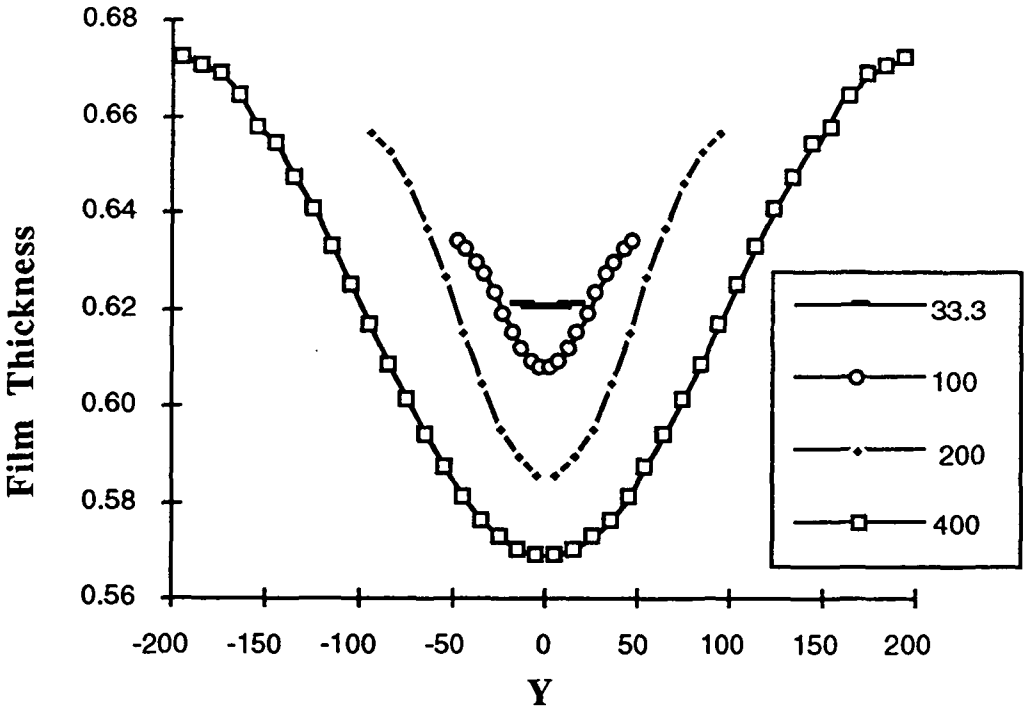

Figure 9. Comparison of the spanwise film thickness profile for pressure variations having spanwise wavelengths of 33.3 (1 mm), 100 (3 mm), 200 (6 mm), and 400 (12 mm) for cases 2,3 5, and 10 of Miura and Aidun (1992), respectively.

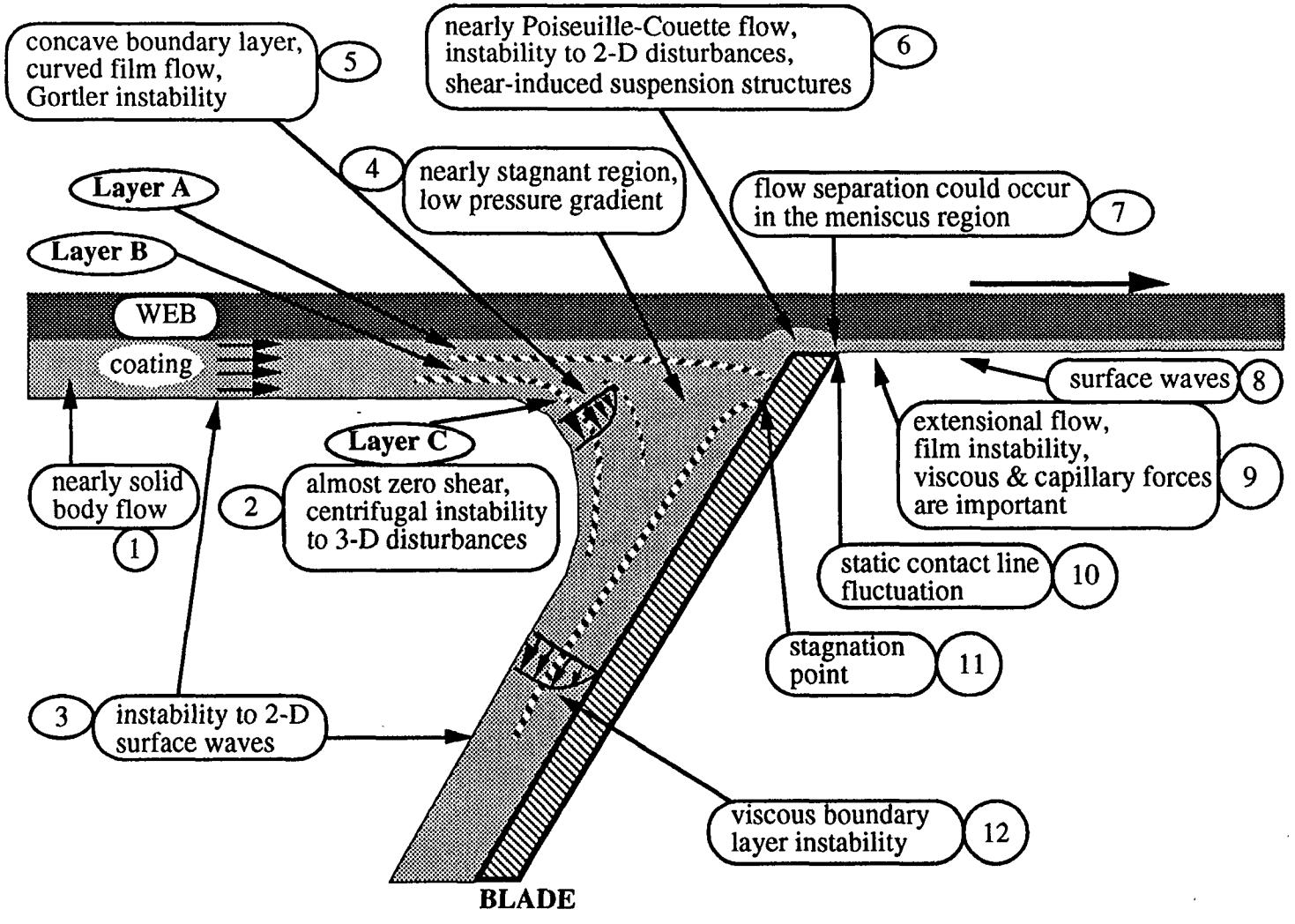

Figure 10. Stability characteristics of flow in blade coating with a roll applicator (see Pranckh and Scriven, 1988 and Miura and Aidun, 1992 for quantitative information).

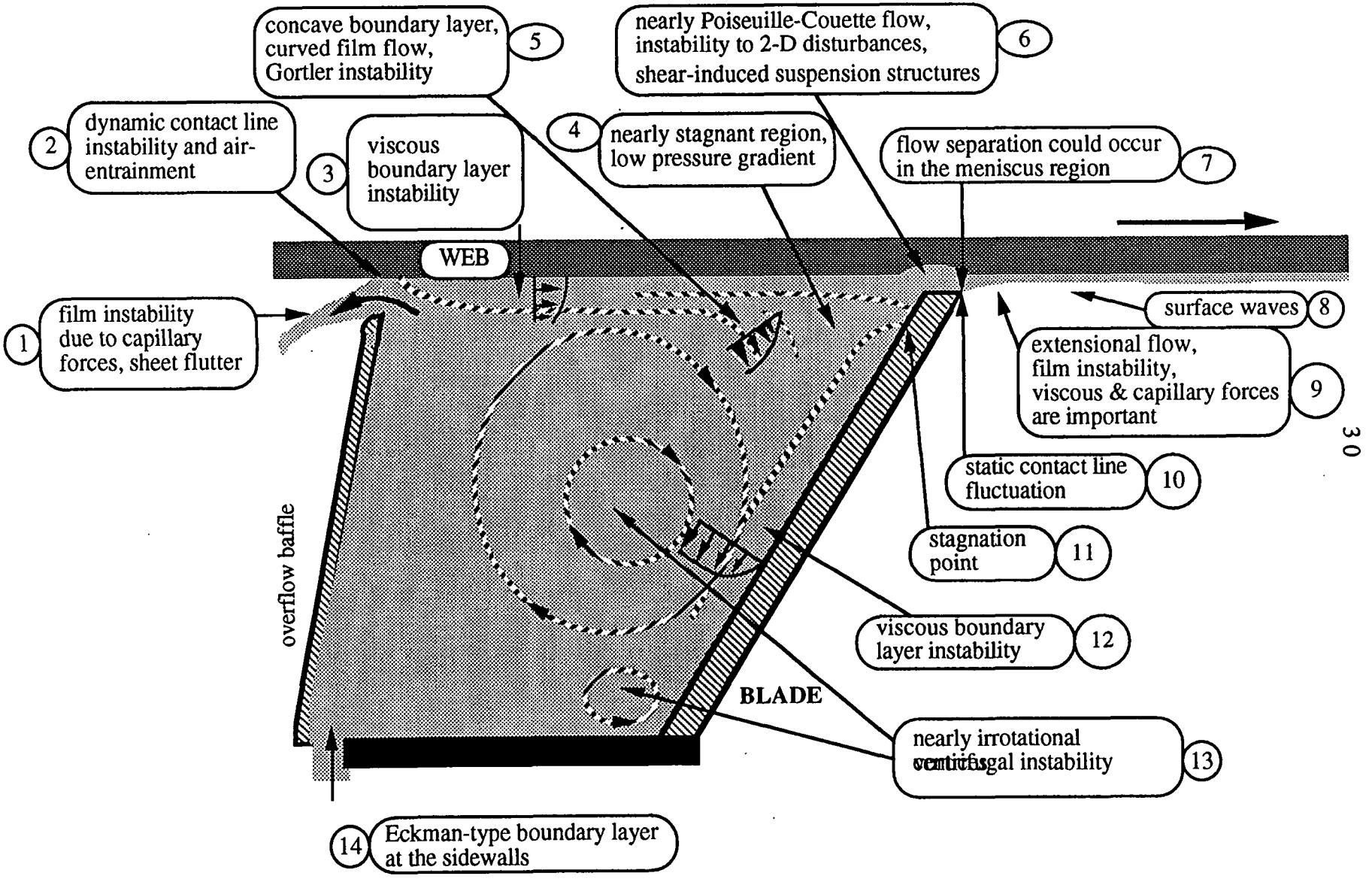

Figure 11. Stability characteristics of flow in blade coating with short-dwell applicator.